Eur. Phys. J. C 50, 857–869 (2007)
DOI 10.1140/epjc/s10052-007-0248-0

THE EUROPEAN PHYSICAL JOURNAL C

Regular Article – Theoretical Physics

On the $d_T = 0$ toy model in reggeon field theory

M.A. Braun[1], G.P. Vacca[2,a]

[1] St. Petersburg State University, St. Petersburg, Russia
[2] INFN and Department of Physics, Via Irnerio 46, Bologna, Italy

Received: 14 December 2006 / Revised version: 24 January 2007 /
Published online: 15 March 2007 –

Abstract. Reggeon field theory with zero transverse dimensions is critically reanalyzed in the Hamiltonian formulation for both a sub- and a supercritical pomeron. Different mathematical aspects of the model, starting from the scalar products in the space of quantum states, are discussed. The probabilistic picture is addressed in the absence of pomeron merging. The issue of the large loop approximation is discussed in terms of the Hamiltonian evolution and its relation to the probabilistic picture recalled. A perturbative treatment, based on the PT symmetry of the model, is proposed that may be useful for more realistic models. Finally, we present numerical calculations for the various parameters of the models, $\alpha(0) - 1 = \mu$ and the triple-pomeron coupling constant λ, which help one to understand some mathematical aspects and the different approximation regimes. They show that the triple-pomeron interaction always makes amplitudes fall with rapidity, irrespective of the value of the intercept. The smaller the values of the ratio λ/μ, the higher are the rapidities y at which this fall starts, so that at small values of λ it begins at asymptotically high rapidities (for $\lambda/\mu < 1/4$ the fall is noticeable only at $\mu y > 100$). No visible singularity is seen for the critical pomeron.

1 Introduction

At high energies quantum chromodynamics tells us that the particle interaction may be mediated by the exchange of hard pomerons, which are non-local entities propagating according to the Balitskii–Fadin–Kuraev–Lipatov (BFKL) equation and splitting into two or merging from two to one, with the known triple-pomeron vertices. This most complicated picture can be drastically simplified in the quasi-classical treatment supposedly valid when at least one of the colliding hadrons is a heavy nucleus. This leaves only tree diagrams, which can be summed by comparatively simple equations, which at least admit a numerical solution. However, at present much attention is paid to the contribution of loops. This is obviously a problem of a completely different level of complexity, since it amounts to solving a full-fledged non-local quantum field theory. At present not even a solution of some local quantum field theory is known except for the one-dimensional case. Naturally, for the study of loops in QCD a one-dimensional model has recently been chosen as a starting point.

The model with zero transverse dimensions, $d_T = 0$ (called the "toy" model) for the dipole picture in QCD was proposed and solved by Mueller [1]. The issue of loop contributions in the dipole picture in QCD was addressed also for a particular zero-dimensional toy model [2] using a probabilistic interpretation, and recently the general issue of loop contributions has attracted much attention.

However, much earlier a model similar in structure was extensively studied in the framework of local reggeon field theory (RFT) in a series of papers [3–9]. As expected, the one-dimensional reduction of the RFT admitted a more or less explicit solution and led to definite predictions as to the behavior of amplitudes both for the hA and AB interaction (of course with the understanding of this being a highly artificial physical picture, very far from the realistic world). In the course of this study many ingenious tricks and techniques were employed and the underlying complicated dynamics was revealed. However, some subtle points have remained unclear in our opinion. In particular the nature of the correspondence between the functional and Hamiltonian approaches and the origin of the restrictions on the form of the wave function and the range of its variables have not been fully exposed.

To elucidate these points is the primary aim of this note. We also try to follow the line presented in [10, 11] to relate the RFT with the probabilistic parton picture for the case when there is no merging of the pomerons (fan diagrams). This gives us an opportunity to discuss within this model the contribution from the loops with the highest extension in rapidity just by joining two fans propagating from the projectile and target towards the center. We additionally develop a perturbation theory for small λ to compute the evolution by noting the PT symmetry of the model. We include also some numerical results in solving the RFT with all loops, which can be obtained quite easily by integrating the corresponding evolution equations.

Note that we exclusively study a model with the triple-pomeron interaction. A different model which additionally

[a] E-mail: Gianpaolo.Vacca@bo.infn.it

includes a quartic pomeron interaction with a particular fine-tuned value of the coupling constant has recently received enough attention in the literature [10–13]. In our opinion the quartic interaction has no immediate counterpart in a realistic pomeron theory with a large number of colors, N_c, where it is damped by a factor $1/N_c^2$.

The paper is organized as follows. The next two sections are devoted to a rigorous formulation of the toy RFT model. A considerable part of their content is not original and can be found scattered over a series of old papers as mentioned above (Sect. 2, 3.1–3.3). It is introduced for clarity and to fix our notation. Some original results are contained in Sect. 3.4 and 3.5. Section 4 is devoted to the simplified case with no pomeron merging. Here, some properties of the wave function and the probabilistic treatment are discussed. In Sect. 5 the results of Sect. 4 are used to discuss an approximation to calculate the contribution of loops by joining two sets of fan diagrams. Section 6 is dedicated to an original perturbative approach based on the PT symmetry of the pomeron Hamiltonian. Finally, in Sect. 7 we present our numerical calculations, which include all the pomeron loop contributions, and we compare them to the various approximations discussed.

2 Functional integral formulation

The toy model of the pomeron interaction with a zero-dimensional transverse space can be defined by the generating functional

$$Z = \int D\phi D\phi^\dagger \, \mathrm{e}^{-S} \,, \tag{1}$$

where

$$S = \int \mathrm{d}y \mathcal{L} \,, \tag{2}$$

and

$$\mathcal{L} = \frac{1}{2}(\phi^\dagger \phi_y - \phi_y^\dagger \phi) - \mu \phi^\dagger \phi + \mathrm{i}\lambda \phi^\dagger \phi (\phi^\dagger + \phi) - \mathrm{i}(j_0 \, \phi^\dagger + j_Y \, \phi) \,. \tag{3}$$

Here μ is the pomeron intercept, $(\alpha(0) - 1)$. For the supercritical pomeron $\mu > 0$. The triple-pomeron coupling constant λ is also positive. The sources $j_0 = \delta(y) g_1$ and $j_Y = \delta(y - Y) g_2$ represent the interaction with the target and projectile, respectively. In the real world $g_1 = g_1(b) = AgT_A(b)$ and $g_2 = g_2(b) = BgT_B(b)$, where g is the pomeron–nucleon coupling constant, A and B are the atomic numbers of the colliding nuclei and T_A and T_B their profile functions.

The functional integral (1) converges for $\mu < 0$, provided the two field variables ϕ and $\phi^\dagger$ are complex conjugates to one another. In fact, putting $\phi = \phi_1 + \mathrm{i}\phi_2$ and $\phi^\dagger = \phi_1 - \mathrm{i}\phi_2$, with both $\phi_{1,2}$ real, we find that all terms in the Lagrangian (3) are pure imaginary, except for the mass term proportional to $\phi^\dagger \phi = \phi_1^2 + \phi_2^2 \geq 0$. So the integrand in (1) contains a factor $\exp\left(\mu \int \mathrm{d}y \left(\phi_1^2 + \phi_2^2\right)\right)$, which guarantees convergence if $\mu < 0$ and the integration over the fields ϕ_1 and ϕ_2 goes over the real axis. For $\mu > 0$ the integral does not exist. Note that the integral does not exist for any sign of μ either if one changes the integration contour in ϕ_1 and ϕ_2, and so over ϕ and $\phi^\dagger$. This means that it is impossible to pass to new fields $u = \mathrm{i}\phi^\dagger$ and $v = \mathrm{i}\phi$ and take u and v real directly in the functional integral as in [5], since it requires an unlawful rotation of the integration contour in the integration over ϕ_1.

Obviously the functional formulation can serve only to define the model for the subcritical pomeron with $\mu < 0$. To define the theory for positive values of μ one has to take recourse to analytic continuation in μ. Note that the properties of the functional integral make one think that there is a singularity at $\mu = 0$. In a fully dimensional RFT it was conjectured that this singularity was related to a phase transition. However, already in [8] it was argued that there was no phase transition in the zero-dimensional world and the amplitudes were analytic in μ on the whole real axis. As we shall see by direct numerical calculation, there is indeed no singularity at $\mu = 0$ in the scattering amplitudes.

In fact the functional formulation is only supported by the fact that it reproduces the perturbative diagrams for the pomeron propagation and interaction. In the following section we introduce an alternative, Hamiltonian formalism, which gives rise to the same perturbative diagrams (an approach taking such as a starting point was briefly mentioned in [6]). However, in contrast to the functional approach it does not involve any limitation on the value or sign of the intercept μ. Since for $\mu < 0$ the perturbative series seems to be convergent, the two formulations are completely equivalent for the subcritical pomeron. Therefore, the Hamiltonian formulation gives the desired analytic continuation of the model to positive values of μ.

3 Hamiltonian formulation

3.1 Basic definitions

Forgetting the functional integral (1) altogether, we now start from a quasi-Schroedinger equation in the rapidity,

$$\frac{\mathrm{d}\Psi(y)}{\mathrm{d}y} = -H\Psi(y) \tag{4}$$

and postulate the form of the Hamiltonian H

$$H = -\mu \phi^\dagger \phi + \mathrm{i}\lambda \phi^\dagger (\phi + \phi^\dagger)\phi \tag{5}$$

as a function of two Hermitean conjugate operators ϕ and $\phi^\dagger$, with the commutator

$$[\phi, \phi^\dagger] = 1 \,. \tag{6}$$

The Hamiltonian is obviously non-Hermitean. In a standard way we split it into free and interaction parts:

$$H = H_0 + H_\mathrm{I}, \quad H_0 = -\mu \phi^\dagger \phi, \quad H_\mathrm{I} = \mathrm{i}\lambda \phi^\dagger (\phi + \phi^\dagger)\phi \,. \tag{7}$$

The next step is to define the physical observables in this picture. In accordance with the commutation relation (6), we define the vacuum state Ψ_0, normalized to unity, by the condition

$$\phi\Psi_0 = 0\,. \tag{8}$$

All other states will be built from Ψ_0 by the application of some numbers of the operator $\phi^\dagger$. We postulate that the transition amplitude from the initial state Ψ_i at rapidity $y = 0$ to the final state Ψ_f at rapidity y is given by

$$\mathrm{i}A_\mathrm{fi} = \langle\Psi_\mathrm{f}|\Psi_\mathrm{i}(y)\rangle = \langle\Psi_\mathrm{f}|\,\mathrm{e}^{-Hy}|\Psi_\mathrm{i}\rangle\ . \tag{9}$$

Here

$$\Psi_\mathrm{i}(y) = \mathrm{e}^{-Hy}\Psi_\mathrm{i} \tag{10}$$

is the initial state evolved to rapidity y. The amplitude A_fi is imaginary positive, so that the matrix element on the right-hand side of (9) is negative.

It will be convenient to define the initial and final states in terms of some operators acting on the vacuum state

$$\Psi_\mathrm{i} = F_\mathrm{i}(\phi^\dagger)\Psi_0, \quad \Psi_\mathrm{f} = F_\mathrm{f}(\phi^\dagger)\Psi_0\,. \tag{11}$$

This allows one to rewrite the amplitude as a vacuum average

$$\mathrm{i}A_\mathrm{fi} = \left\langle F_\mathrm{f}^*(\phi)\,\mathrm{e}^{-Hy}F_\mathrm{i}(\phi^\dagger)\right\rangle, \tag{12}$$

where we do not explicitly write the vacuum state Ψ_0 in which the average is taken.

3.2 Perturbative expansion

We are going to prove that the perturbative expansion of this theory leads to the same Feynman diagrams as obtained in the functional approach. To this end we write

$$\mathrm{i}A_\mathrm{fi} = \left\langle \mathrm{e}^{H_0y}F_\mathrm{f}^*(\phi)\,\mathrm{e}^{-H_0y}\,\mathrm{e}^{H_0y}\,\mathrm{e}^{-Hy}F_\mathrm{i}(\phi^\dagger)\right\rangle\ . \tag{13}$$

From (6) it follows that

$$\phi(y) \equiv \mathrm{e}^{H_0y}\phi\,\mathrm{e}^{-H_0y} = \mathrm{e}^{\mu y}\phi\,. \tag{14}$$

The operator

$$U(y) \equiv \mathrm{e}^{H_0y}\,\mathrm{e}^{-Hy} \tag{15}$$

satisfies the equation

$$\begin{aligned}\frac{\mathrm{d}U(y)}{\mathrm{d}y} &= \mathrm{e}^{H_0y}(H_0 - H)\,\mathrm{e}^{-H(y)}\\ &= -\,\mathrm{e}^{H_0y}H_i\,\mathrm{e}^{-H_0y}U(y)\\ &= H_\mathrm{I}(y)U(y)\,,\end{aligned} \tag{16}$$

where $H_\mathrm{I}(y)$ is the interaction in the interaction representation:

$$H_\mathrm{I}(y) = \mathrm{e}^{H_0y}H_\mathrm{I}(\phi,\phi^\dagger)\,\mathrm{e}^{-H_0y} = H_\mathrm{I}(\phi(y),\phi^\dagger(y))\,, \tag{17}$$

with the rapidity dependent operators (14) and

$$\phi^\dagger(y) \equiv \mathrm{e}^{H_0y}\phi^\dagger\,\mathrm{e}^{-H_0y} = \mathrm{e}^{-\mu y}\phi^\dagger. \tag{18}$$

Note that at $y > 0$ the operators $\phi(y)$ and $\phi^\dagger(y)$ are no more Hermitean conjugates to each other, since the normal time is changed to the imaginary one. However, the similarity transformations (14) and (18) do not change the commutation relations. The solution of (16) with the obvious initial condition $U(0) = 1$ is standard:

$$U(y) = T_y \exp\Big\{-\int_0^y \mathrm{d}y' H_i(y')\Big\}, \tag{19}$$

where T_y means ordering the operators from left to right according to decreasing y. So we get the expression for the amplitude:

$$\mathrm{i}A_\mathrm{fi} = \left\langle F_f^*(\mathrm{e}^{\mu y}\phi)T_y \exp\Big\{-\int_0^y \mathrm{d}y' H_i(y')\Big\}F_\mathrm{i}(\phi^\dagger)\right\rangle\ . \tag{20}$$

Expansion of the expression $T_y \exp$ gives rise to standard Feynman diagrams. The vertices for pomeron splitting and merging will be given by the expected factors $\mathrm{i}\lambda$. The pomeron propagator will be given by

$$P(y_1 - y_2) = \left\langle T_y\Big\{\phi(y_1),\phi^\dagger(y_2)\Big\}\right\rangle = \mathrm{e}^{\mu(y_1-y_2)}\theta(y_1 - y_2)\,, \tag{21}$$

which is the correct pomeron propagator in our toy model. So indeed the theory defined by this Hamiltonian formulation gives rise to standard Feynman diagrams for the RFT.

Note that the Hamiltonian formulation is based on the evolution equation in rapidity and does not require the intercept μ to have a definite sign. It looks equally good both for positive and negative values of μ. For negative μ it produces a perturbative expansion that is identical to the one in the functional approach. So it gives the desired analytic continuation of the functional approach to the region of positive μ, where the latter makes no sense anymore.

3.3 Passing to a real Hamiltonian

It is perfectly possible to continue with the originally defined Schroedinger operators ϕ and $\phi^\dagger$, which are Hermitean conjugates to each other, and satisfy the commutation relation (6). However, it is convenient to pass to new operators u and v in terms of which all ingredients of the theory become real. Following the old papers (starting from [4]) we define

$$u = \mathrm{i}\phi^\dagger, \quad v = \mathrm{i}\phi\,. \tag{22}$$

The new fields are anti-Hermitean to each other

$$u^\dagger = -v, \quad v^\dagger = -u \tag{23}$$

and satisfy the commutation relation

$$[v,u] = -1. \tag{24}$$

However, $v\Psi_0 = 0$, and the states are generated by the action of u. So v is the annihilation and v is the creation operator with the abnormal commutation relation (24).

In terms of new fields the Hamiltonian becomes real:

$$H = \mu uv - \lambda u(u+v)v\,. \tag{25}$$

It is important that also the operators creating the initial and final states become real. It is normally assumed that for the scattering of two nuclei the initial and final wave functions should correspond to the eikonal picture. In terms of the creation operator u, this leads to

$$\Psi_{\mathrm{i(f)}} = F_{\mathrm{i(f)}}(u)\Psi_0, \quad F_{\mathrm{i(f)}}(u) = 1 - \mathrm{e}^{-g_{\mathrm{i(f)}}u}\,. \tag{26}$$

So the expression for the amplitude is rewritten in terms of real quantities:

$$\begin{aligned} \mathrm{i}A_{\mathrm{fi}} &= \left\langle F_{\mathrm{f}}(u)\Psi_0 | \mathrm{e}^{-Hy} | F_{\mathrm{i}}(u)\Psi_0 \right\rangle \\ &= \left\langle \Psi_0 | F_{\mathrm{f}}^*(-v)\,\mathrm{e}^{-Hy} F_{\mathrm{i}}(u)\Psi_0 \right\rangle \\ &= \left\langle \left(1 - \mathrm{e}^{-g_{\mathrm{f}}v}\right)\mathrm{e}^{-Hy}\left(1 - \mathrm{e}^{-g_{\mathrm{i}}u}\right)\right\rangle\,. \end{aligned} \tag{27}$$

Since $H\Psi_0 = 0$, the term independent of g_i and g_f vanishes, so that we can also write

$$\begin{aligned} \mathrm{i}A_{\mathrm{fi}} &= -\left\langle \mathrm{e}^{-g_{\mathrm{f}}v}\,\mathrm{e}^{-Hy}\left(1 - \mathrm{e}^{-g_{\mathrm{i}}u}\right)\right\rangle \\ &= -\left\langle \Psi_0 | \,\mathrm{e}^{-g_{\mathrm{f}}v} F_{\mathrm{i}}(y,u)\Psi_0 \right\rangle, \end{aligned} \tag{28}$$

where $F_{\mathrm{i}}(y,u)$ is the operator that creates the evolved initial state. Since

$$\Psi_{\mathrm{i}}(y) = \mathrm{e}^{-Hy}\Psi_{\mathrm{i}} = \mathrm{e}^{-Hy}F_{\mathrm{i}}(u)\Psi_0 \equiv F_{\mathrm{i}}(y,u)\Psi_0\,, \tag{29}$$

we have

$$\frac{\partial F_{\mathrm{i}}(y,u)}{\partial y} = -H(u,v)F_{\mathrm{i}}(y,u)\,, \tag{30}$$

with the initial condition

$$F_{\mathrm{i}}(0,u) = 1 - \mathrm{e}^{-g_{\mathrm{i}}u}\,. \tag{31}$$

The commutation relation (24) allows one to represent

$$v = -\frac{\partial}{\partial u} \tag{32}$$

and then (28) implies that to find the amplitude one has to substitute u by f_{g} in $F_{\mathrm{i}}(y,u)$:

$$\mathrm{i}A_{\mathrm{fi}} = -F_{\mathrm{i}}(y, g_{\mathrm{f}})\,. \tag{33}$$

This gives a practical recipe for the calculation of the amplitude. One has to solve (30) with the Hamiltonian (25) in which v is represented according to (32):

$$H = -\mu u\frac{\partial}{\partial u} + \lambda u^2\frac{\partial}{\partial u} - \lambda u\frac{\partial^2}{\partial u^2} \tag{34}$$

and the initial condition (31). After the solution is found, one has to substitute u by g_{f} in it.

3.4 Target–projectile symmetry

Taking the complex conjugate of (28) we find

$$\begin{aligned} -\mathrm{i}A_{\mathrm{fi}}^* &= \left\langle \left(1 - \mathrm{e}^{g_{\mathrm{i}}v}\right)\mathrm{e}^{-H^\dagger y}\left(1 - \mathrm{e}^{g_{\mathrm{f}}u}\right)\right\rangle \\ &= \mathrm{i}A_{\mathrm{if}}(\lambda \to -\lambda, g_{\mathrm{i(f)}} \to -g_{\mathrm{f(i)}})\,. \end{aligned} \tag{35}$$

Having in mind that the amplitude is pure imaginary, we see that interchanging the target and projectile leads to changes of sign in the triple-pomeron coupling and the couplings to the external particles. On the other hand changing $u \to -u$ in (30) with the Hamiltonian (34) and the initial condition (31) and also changing signs of λ and g_{i} obviously does not change the solution

$$F_{\mathrm{i}}(y, -u, -g_{\mathrm{i}}, -\lambda) = F_{\mathrm{i}}(y, u, g_{\mathrm{i}}, \lambda)\,, \tag{36}$$

from which we find

$$F_{\mathrm{i}}(y, -g_{\mathrm{f}}, -g_{\mathrm{i}}, -\lambda) = F_{\mathrm{i}}(y, g_{\mathrm{f}}, g_{\mathrm{i}}, \lambda)\,. \tag{37}$$

So the interchange of the target and projectile does not change the amplitude.

3.5 Scalar products

As it follows from our derivation, the exact mathematical realization of the scalar product in the space of wave functions Ψ is irrelevant for the resulting formulas. The representation of the operator v as a minus derivative in u serves only to express its algebraic action on the operator u in accordance with the commutation relation. It does not require one to introduce a representation for the wave function Ψ in which u is represented as multiplication by a complex number, and correspondingly the scalar product is defined by means of integration over the whole complex plane u with a weight factor e^{-uu^*} as in [8]. One may instead represent the operators u and v in terms of the standard Hermitean operators p and q by

$$u = \frac{\mathrm{i}}{\sqrt{2}}(q - \mathrm{i}p), \quad v = \frac{\mathrm{i}}{\sqrt{2}}(q + \mathrm{i}p) \tag{38}$$

and define a scalar product by

$$\langle \Psi_1 | \Psi_2 \rangle = \int \mathrm{d}q \Psi_1^*(q)\Psi_2(q)\,, \tag{39}$$

with $p = -\mathrm{i}\partial/\partial q$. The vacuum state Ψ_0 will be given by the oscillator ground state in this representation.

However, this is not the end of the story. New aspects arise in the process of the solution of (30) for F_{i}. The equation itself is regular everywhere, except possibly at $u = 0$, where, however, it also shows regular behavior for F_{i} constant or linear in u. We are obviously interested in the latter behavior, since from the equation it follows that $F_{\mathrm{i}}(y, u = 0) = 0$. So, in principle, our solution turns out to be regular in the whole complex u-plane. Formally this means that one may choose any continuous interval in this plane and evolve the initial function given in this interval

up to the desired rapidity values. The immediate problem is what interval one has to choose. The final expression for the amplitude requires the value of g_{f} to belong to this interval. In particular for positive g_{f}, the interval should include at least a part of the positive axis.

Numerical calculations show that it is indeed possible to find a solution to the evolution equation, provided the initial interval is restricted to only positive values of u (including the desired value $u=g_{\mathrm{f}}$).

To understand this phenomenon one has to recall some results from the earlier studies. It was found in [6] that there exists a transformation of both the function and variable that converts the non-Hermitean Hamiltonian (34) into a Hermitean one. However, this is only possible for values of u covering the positive axis rather than the whole real axis, where the equation should hold. Namely, one introduces the variable x by

$$u=x^2>0 \tag{40}$$

and makes a similarity transformation of the Hamiltonian

$$\widetilde{H}=W^{-1}HW,\quad W(x)=\sqrt{x}\,\mathrm{e}^{\frac{1}{4}x^4-\frac{\mu}{2\lambda}x^2} \tag{41}$$

to find the transformed Hamiltonian:

$$\widetilde{H}=\frac{\lambda}{4}\Big(-\frac{\partial^2}{\partial x^2}+\frac{3}{4x^2}+x^2(x^2-\varrho)^2-2x^2\Big)\,, \tag{42}$$

where in a standard way we denote $\varrho=\mu/\lambda$. The Hamiltonian $\widetilde{H}$ is a well defined Hamiltonian on the whole real axis with a singularity at $x=0$. The interaction potential infinitely grows at $|x|\to\infty$. So, restricting ourselves to $x>0$ and requiring the eigenfunctions to vanish at the origin and at $x\to\infty$, one finds a discrete spectrum, starting from a certain ground state E_0 going up to infinity. The transformed initial function

$$\widetilde{F}_{\mathrm{i}}(y=0,x)=\frac{1}{\sqrt{x}}\,\mathrm{e}^{-\frac{1}{4}x^4+\frac{\mu}{2\lambda}x^2}\left(1-\mathrm{e}^{-g_{\mathrm{i}}x^2}\right) \tag{43}$$

is well behaved both at $x=0$ and $x=\infty$, and at $0<x<\infty$ it can be expanded in a complete set of eigenfunctions $\widetilde{F}_n$ of $\widetilde{H}$:

$$\widetilde{F}_{\mathrm{i}}(y=0,x)=\sum_{n=0}\Big\langle\widetilde{F}_{\mathrm{i}}(y=0,x)|\widetilde{F}_n\Big\rangle\,\widetilde{F}_n(x)\,. \tag{44}$$

Here a new scalar product has been introduced for the transformed functions:

$$\Big\langle\widetilde{F}_1|\widetilde{F}_2\Big\rangle=\int_0^\infty \mathrm{d}x\widetilde{F}_1^*(x)\widetilde{F}_2(x)\,. \tag{45}$$

Evolution immediately gives

$$\widetilde{F}_{\mathrm{i}}(y,x)=\sum_{n=0}\Big\langle\widetilde{F}_{\mathrm{i}}(y=0,x)|\widetilde{F}_n\Big\rangle\,\mathrm{e}^{-E_n y}\widetilde{F}_n(x)\,, \tag{46}$$

and applying the operator W one finds the solution

$$F(y,u)=\sum_{n=0}\Big\langle\widetilde{F}_{\mathrm{i}}(y=0,x)|\widetilde{F}_n\Big\rangle\,\mathrm{e}^{-E_n y}W(x)\widetilde{F}_n(x)\,,\qquad u=x^2\,. \tag{47}$$

Note that we could just as well start from negative values of u and define instead of (40)

$$u=-x^2,\quad x>0\,. \tag{48}$$

Doing the same transformation of the Hamiltonian we then obtain (42) with the opposite overall sign and an opposite sign of ϱ; that is, the transformed Hamiltonian is now $-\widetilde{H}(\varrho\to-\varrho)$. All eigenvalues now are negative and go down to $-\infty$. If we take the expansion of the initial function analogous to (44) and try to evolve it, we obtain a sum with infinitely growing exponentials in y. Obviously such an evolution makes no sense. This explains why with the positive or negative signs of λ and of the g one can start the evolution only from correspondingly positive or negative values of u, but never from intervals including both.

Also, note that, considered as a function of u, the eigenfunctions are analytic in the whole u-plane. Starting from, say, $u>0$, their values at $u<0$ can be obtained by analytic continuation to pure imaginary values of the variable x. Obviously eigenfunctions should exponentially grow as $u\to-\infty$ (otherwise we shall find positive eigenvalues of the continued Hamiltonian $-\widetilde{H}(\varrho\to-\varrho)$). Similarly, starting from $u<0$ and passing to positive u, one finds that the eigenfunctions exponentially grow at large positive u. So, considering the initial Hamiltonian H on the whole real u axis we find that its spectrum goes from $-\infty$ to $+\infty$ with eigenfunctions that vanish only either at large positive u for positive eigenvalues or at large negative u for negative eigenvalues and exponentially grow otherwise. This prevents us from the introduction of the Bargmann scalar product with integration over the whole complex u-plane.

Finally, let us investigate the qualitative behavior of the system in the large $\lambda/\mu=1/\varrho$ limit, which may be of interest in the generalization to more dimensions, where the effective λ is (infinitely) large [7]. For this purpose, the representation given in (42) is convenient, since it admits a perturbative expansion in ϱ. In the limit $\varrho=0$ one has

$$\widetilde{H}=\frac{\lambda}{4}\Big(-\frac{\partial^2}{\partial x^2}+\frac{3}{4x^2}+x^6-2x^2\Big)\,, \tag{49}$$

which means that the amplitude will behave as e^{-yE_0}, where E_0 is the ground state energy of $\widetilde{H}$. One can perform a semiclassical estimation of the ground state of the Hamiltonian in (49) by imposing the condition

$$\int_{x_1(4E/\lambda)}^{x_2(4E/\lambda)}\mathrm{d}x\sqrt{4E/\lambda-V(x)}=\left(n+\frac{1}{2}\right)\pi\,, \tag{50}$$

where $V(x)=\frac{3}{4x^2}+x^6-2x^2$, and where the x_i are the positive real solutions of the equation $V(x)=4E/\lambda$. For $n=0$ one obtains $E_0\simeq 3.7\lambda/4>0$, which is in very good agreement with the results of the numerical evolution for $\lambda/\mu\geq 3$, which indeed shows decay of the amplitude as e^{-yE_0} after a short initial period of evolution.

Note that during this initial period one observes a rise of the amplitude, which may seem strange in view of the fact that all eigenvalues of the transformed Hamiltonian (41) are in fact positive. This rise is explained by interference of the different contributions which may enter

with different signs due to the non-unitarity of the similarity transformation (41) from the initial non-Hermitean Hamiltonian.

4 No pomeron fusion: fan diagrams

A drastic simplification occurs if one drops in the Hamiltonian the term corresponding to the fusion of pomerons ("fan-case"):

$$H \to H_{fan} = \mu uv - \lambda u^2 v = -(\mu u - \lambda u^2)\frac{\partial}{\partial u}. \quad (51)$$

Then, as has been known since the appearance of [3], the solution can immediately be obtained in explicit form. With the initial condition (26), one finds

$$F_{\rm fan}(y,u) = 1 - \exp\Big(-g_{\rm i}\frac{\varrho}{1-{\rm e}^{-\mu(y+z)}}\Big) = 1 - \exp\left[-\frac{g_{\rm i}u\,{\rm e}^{\mu y}}{1+\frac{u}{\varrho}\,({\rm e}^{\mu y}-1)}\right]. \quad (52)$$

This solution is evidently non-symmetric in the projectile and target. In practice one considers such an approximation in the study of hA scattering. Then it represents the sum of fan diagrams propagating from the projectile hadron towards the target nucleus. This situation corresponds to the lowest order in $g_{\rm i}$ [3]:

$$F^{hA}_{\rm fan} = \frac{g_{\rm i}u\,{\rm e}^{\mu y}}{1+\frac{u}{\varrho}\,({\rm e}^{\mu y}-1)}\,. \quad (53)$$

We recall that the amplitude is obtained from (52) or (53) by putting $u = g_{\rm f}$.

We note that the solution (53) is not analytic in the whole complex u-plane: it evidently has a pole at some negative value of u, which tends to zero from the negative side as $y \to \infty$. So at least for this solution one cannot formulate a scalar product of Bargmann type with integration over the whole complex u-plane. As we have stressed, the existence of such a scalar product is not at all needed.

In fact, the Hamiltonian $H_{\rm fan}$ has the same spectrum as the free Hamiltonian H_0; see (7). The two Hamiltonians are related by a similarity transformation:

$$H_{\rm fan} = VH_0V^{-1}, \quad V = {\rm e}^{-u^2v/\varrho}. \quad (54)$$

It follows that the eigenvalues of $H_{\rm fan}$ are all non-positive: $E_n = -\mu n$ with $n = 0, 1, 2, \ldots$ However, the amplitudes (52) and (53) do not grow but rather tend to a constant at large y. As seen from the structure of the expressions (52) and (53), this is a result of interference of the contributions with different E_n, which separately grow at high y. One can reproduce the result of the fan evolution using the form in (54) by noting that ${\rm e}^{-yH_0}$ is an operator that shifts the variable $\ln u$ by μ, while V corresponds to a shift in the variable $1/u$ by $1/\varrho$.

The fan evolution is to be compared with the situation with the total Hamiltonian H, whose eigenvalues are all non-negative for the branch with positive u. In this case the solutions generally fall at large y and become nearly constant only at very small λ when one of the excited levels goes down practically to zero due to the particular structure of the transformed Hamiltonian (42) [6]. So the mechanism for the saturation of the amplitudes at large rapidities is completely different for the complete Hamiltonian H and its fan part $H_{\rm fan}$.

Unlike the complete model with fusion [10, 11], the fan case admits a reinterpretation in probabilistic terms, which may turn out to be helpful for applications.

Consider first the case $\mu > 0$. Let us represent a solution $F(y,u)$ by a power series in u:

$$F(y,u) = \sum_{n=1} c_n(y)u^n. \quad (55)$$

We rescale $y = \bar{y}/\mu$ and write

$$c_n(\bar{y}) = \frac{1}{n!}(-\varrho)^{1-n}\nu_n(\bar{y})g_{\rm i}\,. \quad (56)$$

The evolution equation gives a system of equations for ν_n:

$$\frac{{\rm d}\nu_n(\bar{y})}{{\rm d}\bar{y}} = n\nu_n(\bar{y}) + n(n-1)\nu_{n-1}(\bar{y}). \quad (57)$$

This equation is identical with the one that is obtained for the multiple moments of the probability $P_k(\bar{y})$ to have exactly k pomerons:

$$\nu_n(\bar{y}) = \sum_{k=n} P_k(\bar{y})\frac{k!}{(k-n)!}\,, \quad (58)$$

provided the probabilities obey the equation

$$\frac{{\rm d}P_n(\bar{y})}{{\rm d}\bar{y}} = -nP_n(\bar{y}) + (n-1)P_{n-1}(\bar{y}). \quad (59)$$

The equations for P_n are such that they conserve the total probability assumed to be equal to unity. Also if the initial probabilities are non-negative, they will remain so during the evolution. This gives the justification for the interpretation of P_n as probabilities.

The generating functional for the probabilities P_n

$$Z(\bar{y},u) = \sum_n P_n(\bar{y})u^n \quad (60)$$

satisfies the equation

$$\frac{\partial Z(\bar{y},u)}{\partial\bar{y}} = (u^2-u)\frac{\partial Z(\bar{y},u)}{\partial u}\,. \quad (61)$$

Note that this is essentially the same equation as for F with parameters put to unity and the opposite sign of the Hamiltonian. So its solution for a general initial condition is

$$Z(\bar{y},u) = Z\,(0, z(u)-\bar{y})\,, \quad u = \frac{1}{1-{\rm e}^{-z}}\,. \quad (62)$$

For the simple case of hA scattering this gives (c.f. (53) with unit parameters and opposite rapidity)

$$Z^{hA} = \frac{u\,\mathrm{e}^{-\bar{y}}}{1+u(\mathrm{e}^{-\bar{y}}-1)}\,. \tag{63}$$

An expansion in powers of u gives the probabilities P_n:

$$P_n^{hA} = \mathrm{e}^{-\bar{y}}\left(1-\mathrm{e}^{-\bar{y}}\right)^{n-1}. \tag{64}$$

For the general case we first construct $Z(y=0)$ as the sum

$$Z(0,u) = 1+\sum_{n=1}\nu_n(0)\frac{(u-1)^n}{n!} \tag{65}$$

with values of $\nu_n(0)$ known from the initial distribution,

$$\nu_n(0) = (g_\mathrm{i}\varrho)^{n-1}\,. \tag{66}$$

Subsequent summation and the shift $z \to z-\bar{y}$ lead to the final result:

$$Z(\bar{y},u) = 1-\frac{1}{g_\mathrm{i}\varrho}+\frac{1}{g_\mathrm{i}\varrho}\exp\left(g_\mathrm{i}\varrho\frac{(u-1)\,\mathrm{e}^{\bar{y}}}{u-(u-1)\,\mathrm{e}^{\bar{y}}}\right). \tag{67}$$

The probabilities should be obtained by developing this expression around $u=0$, which is not easily done in the general form.

Now let us briefly comment on the case of the subcritical pomeron, $\mu = -\epsilon < 0$. We again rescale

$$y = y'/\epsilon \tag{68}$$

and instead of (56) put

$$c_n(y') = \frac{1}{n!}\varrho^{1-n}\nu_n'(y')g_\mathrm{i}\,, \tag{69}$$

where now $\varrho = -\epsilon/\lambda < 0$. The resulting equations for ν_n' are

$$\frac{\mathrm{d}\nu_n'(y')}{\mathrm{d}y'} = -n\nu_n'(y')+n(n-1)\nu_{n-1}'(y')\,. \tag{70}$$

As we see they become similar to the equations for P_n in the case of $\mu > 0$ and in fact coincide with them for the quantities $\tilde{\nu}_n = \nu_n'/n!$. This means that for negative μ the relation between the RFT and the probabilistic picture is different from the case of positive μ. In fact, the interpretation of the amplitude in terms of P_n and ν_n is interchanged: the rescaled coefficients c_n in the amplitude directly give the probabilities to find a given number of pomerons, and their multiple moments have to be defined in terms of these quantities in a way similar to the construction of probabilities from their moments for $\mu > 0$.

5 Big loops

One can use the Hamiltonian approach to find the contribution of loops with maximal extension in rapidity, similar to the approach first taken in [14] in the fully dimensional dipole picture. This issue has also been investigated for a different model with a specific quartic interaction, in which an exact solution can be built [12]. To this end we first split the evolution in two parts:

$$\begin{aligned}\mathrm{i}A_\mathrm{fi}(y) &= \left\langle F_\mathrm{f}^*(-v)\,\mathrm{e}^{-Hy}F_\mathrm{i}(u)\right\rangle \\ &= \left\langle F_\mathrm{f}^*(-v)\,\mathrm{e}^{-Hy/2}\,\mathrm{e}^{-Hy/2}F_\mathrm{i}(u)\right\rangle \\ &= \left\langle \left(\mathrm{e}^{-H^\dagger y/2}F_\mathrm{f}(u)\right)^\dagger \mathrm{e}^{-Hy/2}F_\mathrm{i}(u)\right\rangle . \end{aligned}\tag{71}$$

Next we neglect the fusion of pomerons during the first part of the evolution and the merging of them during the second part:

$$\mathrm{i}A_\mathrm{fi}(y) = \left\langle \left(\mathrm{e}^{-H_\mathrm{fan}^\dagger y/2}F_\mathrm{f}(u)\right)^\dagger \mathrm{e}^{-H_\mathrm{fan}y/2}F_\mathrm{i}(u)\right\rangle . \tag{72}$$

Here H_fan is given by (51) and $H_\mathrm{fan}^\dagger$ differs from it by the sign of λ. This approximation takes into account loops that are obtained by joining at center rapidity the two sets of fan diagrams going from the target and projectile.

Both operators inside the vacuum average are known and are given by (52) or (53) with the understanding that for the solution with $H_\mathrm{fan}^\dagger$ one has to change the sign of λ. To simplify, we restrict ourselves to the lowest order in both coupling constants, $g_{\mathrm{i(f)}}$. Separating g_i and g_f we then obtain the pomeron Green function with loops of the maximal extension. In this case the right factor in (72) is given by

$$\mathrm{e}^{-H_\mathrm{fan}y/2}u = \frac{u\,\mathrm{e}^{\mu y/2}}{1+\frac{u}{\varrho}\left(\mathrm{e}^{\mu y/2}-1\right)} \tag{73}$$

and the right factor is

$$\begin{aligned}\left(\mathrm{e}^{-H_\mathrm{fan}^\dagger y/2}u\right)^\dagger &= \left[\frac{u\,\mathrm{e}^{\mu y/2}}{1-\frac{u}{\varrho}\left(\mathrm{e}^{\mu y/2}-1\right)}\right]^\dagger \\ &= \frac{-v\,\mathrm{e}^{\mu y/2}}{1+\frac{v}{\varrho}\left(\mathrm{e}^{\mu y/2}-1\right)}\,. \end{aligned}\tag{74}$$

So the pomeron Green function is

$$G(y) = -\left\langle \frac{v\,\mathrm{e}^{\mu y/2}}{1+\frac{v}{\varrho}\left(\mathrm{e}^{\mu y/2}-1\right)}\frac{u\,\mathrm{e}^{\mu y/2}}{1+\frac{u}{\varrho}\left(\mathrm{e}^{\mu y/2}-1\right)}\right\rangle . \tag{75}$$

Its calculation is trivial. Denoting

$$b = \frac{1}{\varrho}\left(\mathrm{e}^{\mu y/2}-1\right), \tag{76}$$

we write the left operator as

$$\frac{v\,\mathrm{e}^{\mu y/2}}{1+\frac{v}{\varrho}\left(\mathrm{e}^{\mu y/2}-1\right)} = \mathrm{e}^{\mu y/2}\frac{v}{1+bv} = \mathrm{e}^{\mu y/2}\frac{1}{b}\left(1-\frac{1}{b}\frac{1}{v+1/b}\right). \quad (77)$$

The action of the unit operator gives zero, so that we are left with

$$G(y) = \mathrm{e}^{\mu y}\frac{1}{b^2}\left\langle \frac{1}{v+1/b}\frac{u}{1+bu}\right\rangle . \quad (78)$$

Now we write

$$\frac{1}{v+1/b} = \int_0^\infty \mathrm{d}x\,\mathrm{e}^{-x(v+1/b)}, \quad (79)$$

and, since the operator e^{-xv} just substitutes u by x in the vacuum average, we obtain

$$G(y) = \mathrm{e}^{\mu y}\frac{1}{b^2}\int_0^\infty \mathrm{d}x\,\mathrm{e}^{-x/b}\frac{x}{1+bx} = \mathrm{e}^{\mu y}\frac{1}{b^2}\left(1+\frac{1}{b^2}\,\mathrm{e}^{1/b^2}\mathrm{Ei}(-1/b^2)\right). \quad (80)$$

In the asymptotic limit $y\to\infty$, in this approximation, the propagator tends to a constant value:

$$G(y)_{y\to\infty} \simeq \varrho^2\frac{\mathrm{e}^{\mu y}}{\left(\mathrm{e}^{\mu y/2}-1\right)^2} \simeq \varrho^2. \quad (81)$$

The loops have tamed its initial exponential growth by $\mathrm{e}^{\mu y}$, illustrating the saturation phenomenon in the old Gribov RFT with the supercritical pomeron.

Note that the same result can be obtained by developing in the number of interactions [14, 15]. We find it worthwhile to remind the reader how one proceeds in this case. In fact, we can expand both wave functions in powers of u and v, respectively, as in (55). Obviously only terms with equal numbers of u and v contribute with

$$\langle v^n u^n\rangle = (-1)^n n!. \quad (82)$$

So we get

$$G(y) = -\sum_{n=1}(-1)^n n! c_n^2(y/2), \quad (83)$$

where from (53) we find

$$c_n(y/2) = \mathrm{e}^{\mu y/2}(-b)^{n-1}. \quad (84)$$

We find a divergent series:

$$G(y) = -\frac{1}{b^2}\,\mathrm{e}^{\mu y}\sum_{n=1}(-b^2)^n n!, \quad (85)$$

which is, however, Borel summable. Representing

$$n! = \int_0^\infty \mathrm{d}t\,\mathrm{e}^{-t}t^n, \quad (86)$$

we get

$$G(y) = -\frac{1}{b^2}\,\mathrm{e}^{\mu y}\int_0^\infty \mathrm{d}t\,\mathrm{e}^{-t}\sum_{n=1}(-b^2t)^n = \mathrm{e}^{\mu y}\int_0^\infty \mathrm{d}t\,\mathrm{e}^{-t}\frac{t}{1+b^2t}. \quad (87)$$

This is the same expression as (80), which we obtained before. So these simple but not very rigorous manipulations give the correct answer.

It is instructive to express the same result in terms of the probabilities P_n. Actually, this is a straightforward task. Rescaling the coefficients c_n in (83), we rewrite this expression in terms of the multiple probability moments ν_n:

$$G(y) = -\varrho^x 2\sum_{n=1}\left(-\frac{1}{\varrho^2}\right)^n \nu_n^2(y/2)\frac{1}{n!}. \quad (88)$$

Now we express the multiple moments in terms of the probabilities according to (58) to finally obtain

$$G(y) = \sum_{k,l=1} P_k(y/2)P_l(y/2)F_{kl}, \quad (89)$$

where F_{kl} are coefficients independent of the energy:

$$F_{kl} = \sum_{n=1} n! C_k^n C_l^n\left(-\frac{1}{\varrho^2}\right)^{n-1}. \quad (90)$$

It is easy to find the asymptotical values of F_{kl} at large k and l. Then we can approximate

$$C_k^n \simeq \frac{k^n}{n!}, \quad n << k\to\infty. \quad (91)$$

In this approximation

$$F_{kl} = -\varrho^2\sum_{n=1}\frac{1}{n!}\Big(-\frac{kl}{\varrho^2}\Big)^n = \varrho^2\Big(1-\mathrm{e}^{-kl/\varrho^2}\Big). \quad (92)$$

Now we get from (88)

$$G(y) = \varrho^2\left(1-\sum_{k,l=1}P_k(y/2)P_l(y/2)\,\mathrm{e}^{-kl/\varrho^2}\right). \quad (93)$$

At high y and fixed n the probabilities $P_n(y)$ become independent of n and become equal to $\mathrm{e}^{-\mu y}$ (see (64)). Then we get

$$G(y) = \varrho^2\left(1-\mathrm{e}^{-\mu y}\sum_{k,l=1}\mathrm{e}^{-kl/\varrho^2}\right), \quad (94)$$

with the correct limiting value ϱ^2 at $y\to\infty$.

6 Perturbative analysis for small λ and PT symmetry

Having in mind possible generalizations to the realistic two-dimensional world, in this section we study the perturbative treatment of the model at small values of λ. As it follows from the previous studies [6–8] actually the point $\lambda=0$ corresponds to an essential singularity in the Hamiltonian spectrum corresponding to the existence of a low-lying excited state with a positive energy:

$$\Delta E=\frac{\mu^2}{\sqrt{2\pi\lambda}}\,\mathrm{e}^{-\varrho^2/2}. \tag{95}$$

This state dominates the evolution at very high rapidities. However at earlier stages of the evolution, this unperturbative component may play a secondary role as compared to purely perturbative contributions. We also point out in this section some general properties of the Hamiltonian H given by (5), which belongs to a class of non-Hermitean Hamiltonians widely studied in the literature.

Inspecting the Hamiltonian H we can see that even if it is not Hermitean, it describes a PT symmetric system evolving in the imaginary time. This property has been intensively studied mainly for anharmonic oscillators [16, 17]. Indeed, H is invariant under the product of parity and "time"-reversal transformations: $\phi\to-\phi$, $\phi^\dagger\to-\phi^\dagger$ and $\mathrm{i}\to-\mathrm{i}$.

As the transformation to the form (42) has shown, the spectrum of H is real. This fact is true whenever for a diagonalizable operator H certain conditions are fulfilled [18, 19]. The most important one is that H should be Hermitean with respect to some positive-definite scalar product $\langle\cdot|\cdot\rangle_\eta=\langle\cdot|\eta\cdot\rangle$, constructed using a metric operator $\eta=\mathrm{e}^{-Q}$ defined to be positive with Hermitean Q. This defines the η-pseudo-Hermiticity property of H, which may conveniently be written

$$H^\dagger=\eta\,H\,\eta^{-1}=\mathrm{e}^{-Q}H\,\mathrm{e}^{Q}. \tag{96}$$

Considering the set all positive-definite metric operators, it is easy to see that the parity operator P belongs to it. Then one can define a C operator by $C=P^{-1}\eta=\eta^{-1}P$ that commutes with the Hamiltonian H and the PT symmetry generator. In this formalism one should therefore introduce as a scalar product the CPT inner scalar product:

$$\begin{aligned}\langle\Psi_1|\Psi_2\rangle_{CPT}&=\left\langle\Psi_1|\,\mathrm{e}^{-Q}\Psi_2\right\rangle\\&=\left\langle\mathrm{e}^{-Q/2}\Psi_1|\,\mathrm{e}^{-Q/2}\Psi_2\right\rangle.\end{aligned} \tag{97}$$

The η operator is in general unique up to symmetries of H. It describes the nature of the physical Hilbert space, the observables being the η-pseudo-Hermitean operators. Using the symmetric (second) form of the scalar product (97), we define

$$h=\mathrm{e}^{-Q/2}H\,\mathrm{e}^{Q/2}, \tag{98}$$

which is Hermitean with respect to the scalar product in this form. The eigenvalues of h and H obviously coincide.

The operator Q can be determined perturbatively. In full generality we write

$$H=H_0+\lambda H_1, \tag{99}$$

and in the perturbative expansion $Q=\lambda Q_1+\lambda^3Q_3+\cdots$ we may derive the terms Q_i using (96) and matching the terms at each order in λ. Here we shall restrict ourselves to the first two orders in perturbation theory:

$$\begin{aligned}\left[H_0,\frac{Q_1}{2}\right]&=-H_1,\\\left[H_0,\frac{Q_3}{2}\right]&=-\frac{1}{3}\left[\left[H_1,\frac{Q_1}{2}\right],\frac{Q_1}{2}\right].\end{aligned} \tag{100}$$

Inserting this into (98) for $h=h^{(0)}+\lambda^2h^{(2)}+\lambda^4h^{(4)}+\cdots$, one obtains

$$\begin{aligned}h^{(0)}&=H_0,\\h^{(2)}&=\frac{1}{2}\left[H_1,\frac{Q_1}{2}\right],\\h^{(4)}&=\frac{1}{2}\left[H_1,\frac{Q_3}{2}\right]+\frac{1}{8}\left[\left[H_0,\frac{Q_3}{2}\right],\frac{Q_1}{2}\right].\end{aligned} \tag{101}$$

Let us now use these results for the system under investigation. We define the operators

$$\begin{aligned}N&=\phi^\dagger\phi,\\R_n&=N^n\phi+\phi^\dagger N^n,\\S_n&=N^n\phi-\phi^\dagger N^n\end{aligned} \tag{102}$$

and write $H_0=-\mu N$ and $H_1=\mathrm{i}R_1$. One easily finds that

$$\begin{aligned}\frac{Q_1}{2}&=-\frac{\mathrm{i}}{\mu}S_1,\\\frac{Q_3}{2}&=\frac{4\mathrm{i}}{\mu^3}\left(S_2+\frac{1}{3}S_1\right).\end{aligned} \tag{103}$$

Finally, inserting these expressions into (101), one obtains for h up to order λ^4

$$\begin{aligned}h=-\mu\Bigg[&N+\frac{\lambda^2}{\mu^2}\left(3N^2-N\right)\\&8+\frac{\lambda^4}{\mu^4}\left(-12N^3+6N^2-2N+\Delta h^{(4)}\right)\\&+\mathcal{O}\left(\frac{\lambda^6}{\mu^6}\right)\Bigg],\end{aligned} \tag{104}$$

where

$$\Delta h^{(4)}=\frac{5}{2}\left(N(N+1)\phi^2+\phi^{\dagger2}N(N+1)\right) \tag{105}$$

is a term not diagonal in the number operator N and thus contributing to the energy eigenvalues only at a higher order in λ/μ.

Note that the transformation (41) for positive u and λ leads to the Hamiltonian (42), which has all eigenvalues positive. In contrast, the perturbative eigenvalues are

seemingly non-positive for small enough λ and certainly so at $\lambda = 0$. This shows that the perturbative series is not convergent. Note, however, that it provides a reasonable asymptotic expansion at small values of λ for not very high rapidities and describes well the initial period of the evolution when the amplitudes rise. As an illustration, using this perturbatively approximated spectrum one may compute the pomeron propagator at two loops, using

$$G(y) = \langle 0|\phi \mathrm{e}^{-yH}\phi^\dagger|0\rangle = \left\langle 0|\phi \mathrm{e}^{Q/2}\,\mathrm{e}^{-yh}\,\mathrm{e}^{-Q/2}\phi^\dagger|0\right\rangle , \quad (106)$$

expanded in the basis $|n\rangle_h$ of the eigenstates of h ($h|n\rangle_h = E_n|n\rangle_h$). Comparison to the exact numerical evolution in the next section shows perfect agreement up to some value of μy, much below the saturation region, beyond which the perturbative approximation, which continues to grow in rapidity, fails. In particular for $\lambda/\mu = 1/10$, the perturbative approximation is very good up to $\mu y \le 3$.

In the limit $\lambda \to 0$ one finds that the initial period of evolution, when the amplitude grows, extends to infinitely high rapidities, and the propagator continuously passes into the free one, growing as $\exp(\mu y)$. So in spite of the essential singularity at $\lambda = 0$, the amplitudes seem to have a well defined limit as $\lambda \to 0$, when they continuously pass into free ones.

One might expect it to be reasonable to apply a similar perturbative approach for some interval of rapidity also in the case for non-zero transverse dimensions.

7 Numerical calculations

As mentioned in the introduction, most of the qualitative results in the toy model were obtained thirty years ago [4–9]. They were restricted to the case of a very small triple-pomeron coupling λ, when the dynamics becomes especially transparent and admits asymptotic estimates. However, the smallness of λ in the zero-dimensional case actually does not correspond to the physical situation in the world with two transverse dimensions. If the transverse space is approximated by a two-dimensional lattice with intersite distance a, then the effective coupling constant in the zero-dimensional world is inversely proportional to a and thus goes to infinity in the continuum space [7]. So the behavior of the model at any values of μ and λ has a certain interest. In particular, it may be interesting to know the behavior at $\mu \to 0$, since the functional integral defining the theory for $\mu < 0$ diverges at $\mu > 0$, and one can expect a certain singularity at $\mu = 0$. The validity of different approximate methods to find the solution may also be of interest in view of applications to more realistic models.

Modern calculational facilities allow one to find solutions for the model at any values of μ and λ without any difficulty. Our approach was to evolve the wave function in rapidity directly from its initial value at $y = 0$ using (30) by the Runge–Kutta technique. This straightforward approach proved to be simple and powerful enough to give reliable results for a very short time. True, the step in rapidity had to be chosen rather small and correlated with the step in u. In practice, we chose the initial interval of u as

$$0 < u < 20 \quad (107)$$

divided in 2000 points. The corresponding step in rapidity had to be taken not greater than 2.5×10^{-3}.

Presenting our results we have in mind that the amplitudes not only depend on the dynamics but also on the two coupling constants $g_{\mathrm{i(f)}}$. To economize we therefore restrict ourselves; we show either the full pomeron propagator

$$P(y) = -\left\langle v \mathrm{e}^{-Hy} u\right\rangle \quad (108)$$

or the amplitude for the process which mimics hadron–nucleus scattering

$$A(y, g) = -\left\langle \mathrm{e}^{-gv}\,\mathrm{e}^{-Hy} u\right\rangle \quad (109)$$

(with $g_{\mathrm{f}} \equiv g > 0$ and $g_{\mathrm{i}} = 1$).

7.1 Pomeron propagator

The straightforward evolution according to (30) from the initial wave function $F_{\mathrm{i}}(0, u) = u$ gives the results for the pomeron propagator shown in Fig. 1 for different sets of μ and λ. We recall that the free propagator is just

$$P_0(y) = \mathrm{e}^{\mu y} . \quad (110)$$

Inspection of the curves in Fig. 1 allows one to draw the following conclusions.

1. Inclusion of the triple-pomeron interaction of any strength makes the propagator fall with rapidity. This fall is the stronger the larger the coupling.
2. At very small values of the coupling ($\varrho \sim 10$ or greater) the fall is not felt at the maximal rapidity $y = 50$ chosen for the evolution. This is in full accord with the

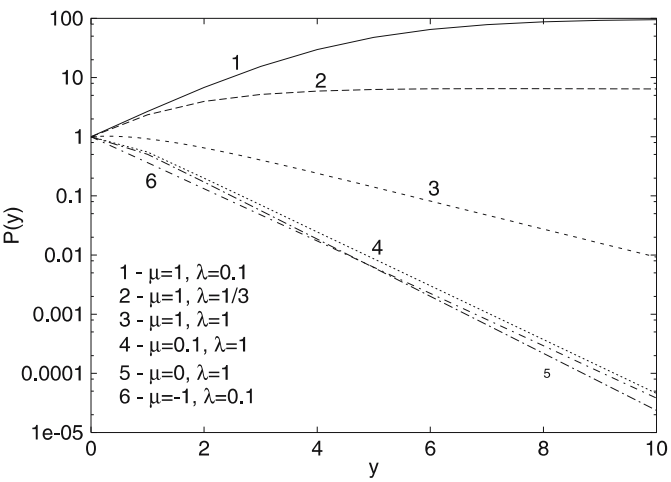

Fig. 1. The full pomeron propagator as a function of rapidity for different sets of μ and λ as indicated in the figure

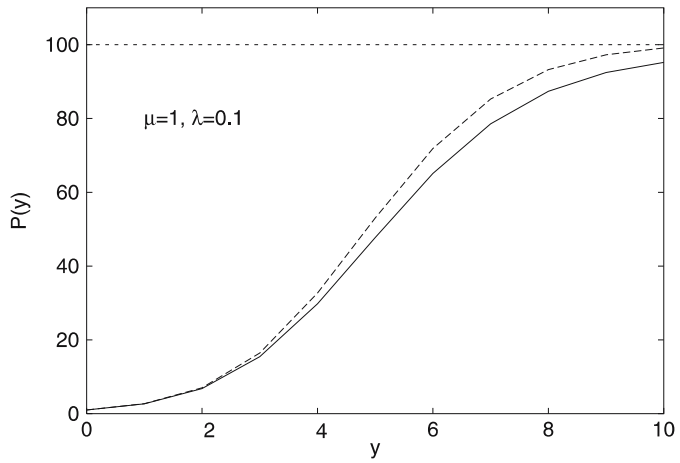

Fig. 2. The full pomeron propagator as a function of rapidity for $\mu=1$ and $\lambda=0.1$ (*lower curve*) as compared to the "big loop" formula (80) (*middle curve*) and the asymptotic expression (111) (*upper curve*)

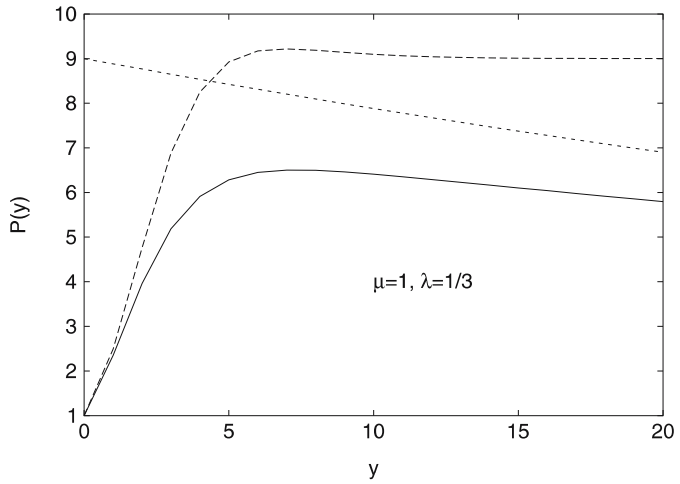

Fig. 3. The full pomeron propagator as a function of rapidity for $\mu=1$ and $\lambda=1/3$ (*lower curve*) as compared to the "big loop" formula (80) (*upper curve on the right*) and the asymptotic expression (111) (*middle curve on the right*)

predictions of earlier studies [6–8], in which it was concluded that the behavior should be $\sim\exp(-\Delta E y)$, with ΔE given by (95). With $\mu=1$ and $\varrho=10$, one finds $\Delta E\sim E-21$, so that the fall of the propagator should be felt only at fantastically large rapidities.

3. However, already with $\mu=1$ and $\lambda=1/3$ the decrease of the propagator with the growth of y is visible (see the non-logarithmic plot in Fig. 3).
4. With small values of μ at $\lambda=1$ the propagator goes down practically as $\exp(-y)$, so that the triple-pomeron coupling takes the role of the damping mechanism.
5. No singularity is visible at $\mu=0$ and fixed $\lambda=1$. The curves with the very small values $\mu=\pm E-4$ look completely identical. Of course, this does not exclude discontinuities in higher derivatives, which we do not see numerically.

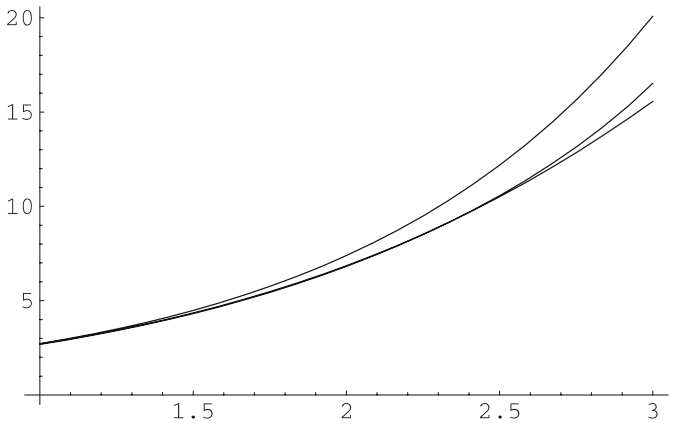

Fig. 4. The pomeron Green function as a function of μy for $\mu=1$ and $\lambda=1/10$. From *bottom* to *top*: the exact numerical evolution, the two loop perturbative approximation and the free case ($\mathrm{e}^{y\mu}$)

We next compared our exact results with two approximate estimates. The first one is the propagator obtained in the approximation of "big loops", (80). The second is the asymptotic expression at small λ obtained in earlier studies,

$$P(y)=\varrho^2\,\mathrm{e}^{-y\Delta E}\,, \tag{111}$$

with ΔE given by (95). The results for $\mu=1$ and $\lambda=1/10$ and $1/3$ are shown in Figs. 2 and 3, respectively. As one observes, both approximations are not quite satisfactory. For quite small $\lambda=1/10$, the asymptotic limit, which we followed up to $y\sim 50$, is correctly reproduced in both approximations. However, the exact propagator seems to reach this limit at still higher values of y (to start falling at fantastically large $y\sim$
$valunit*NumberE20$). The behavior at small values of y is of course not described by (111) at all. The "big loop" approximation works better and describes the rising part of the curve with an error of less than 10%, which goes down to 2% for $y\geq 15$. At larger values of λ the situation becomes worse. As seen from Fig. 3 ($\lambda=1/3$) both approximations work very poorly. The "big loop" approximation fails to reproduce both the magnitude of the propagator and its fall at large y. It describes the propagator more or less satisfactorily only at small values of $y\leq 2$. The approximation (111) describes the trend of the propagator at higher y better but also fails to reproduce its magnitude. For still higher values of λ, both approximations do not work at all. So our conclusion is that both approximations are applicable only at quite small values of $\lambda/\mu<1/5$ and that the approximation of "big loop" is better, since it also reproduces the growth of the propagator at smaller y from its initial value $P(0)=1$ to its asymptotic value ϱ^2 at the maximal rapidities considered.

In Fig. 4 we compare the exact pomeron propagator with the calculations based on the perturbative expansion (up to two loops) and with the free propagator (110). One observes that there exists a region of intermediate values of μy, from 1 to approximately 3, where, on the one hand, the

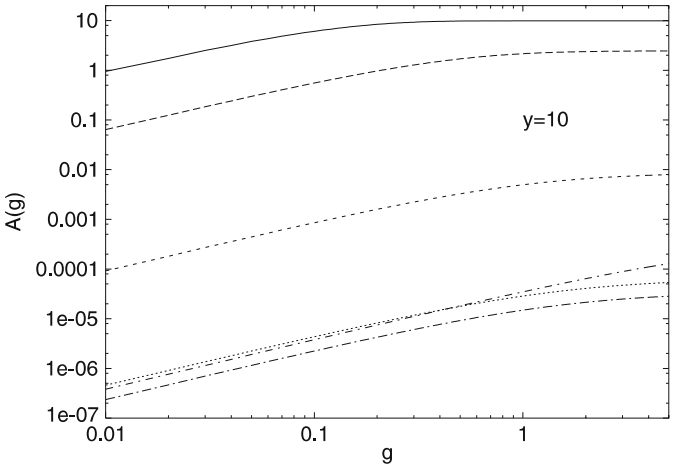

Fig. 5. The hA amplitude at $y=10$ as a function of the coupling to the target. *Curves* from *top* to *bottom* on the right correspond to $(\mu,\lambda)=(1,0.1)$, $(1,1/3)$, $(1,1)$, $(-1,0.1)$, $(0.1,1)$, $(0,1)$

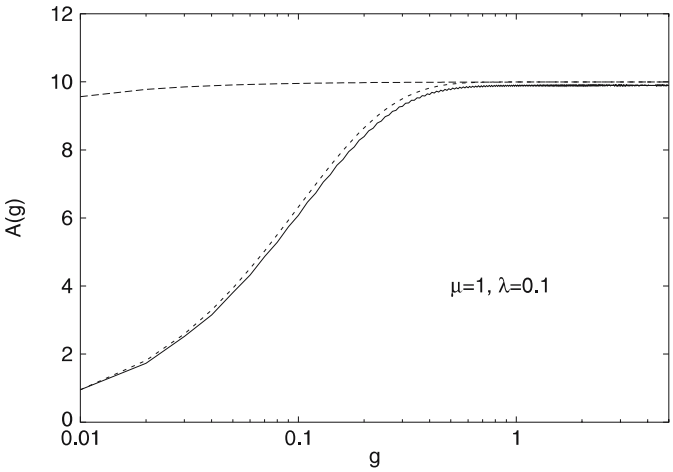

Fig. 6. The hA amplitude $A(y,g)$ at $y=10$ for $\mu=1$, $\lambda=0.1$ (*lower curve*) as compared to the pure fan prediction (*upper curve*) and the asymptotic expression (112) (*middle curve*)

influence of loops is already noticeable and, on the other hand, the perturbative approach works with a reasonable precision.

7.2 hA amplitude

In Fig. 5 we show our results for the amplitude $A(y,g)$ at comparatively large rapidity $y=10$ as a function of the coupling g to the target for different sets of μ and λ. This dependence mimics that of a realistic hA amplitude on the atomic number of the nucleus. In all cases except for $(\mu,\lambda)=(-1,1/10)$, the amplitude $A(g)$ rapidly grows as g rises from zero to approximately unity and then continues to grow very slowly at higher values of g, clearly showing signs of saturation. To make this behavior visible we use a log–log plot. In the exceptional case $(\mu,\lambda)=(-1,1/10)$ one

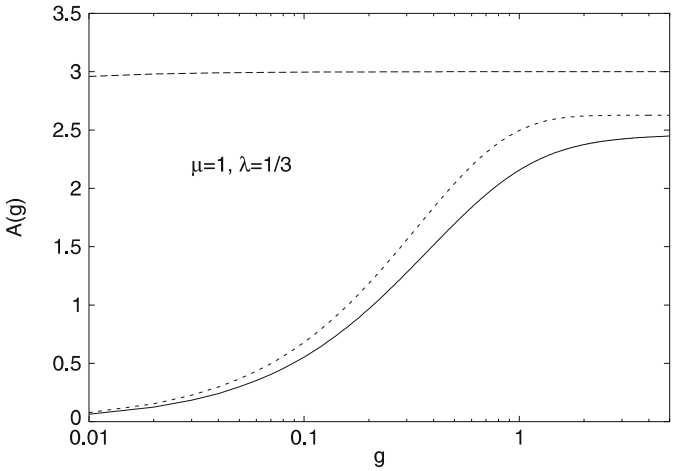

Fig. 7. Same as Fig. 5 for $\mu=1$ and $\lambda=1/3$

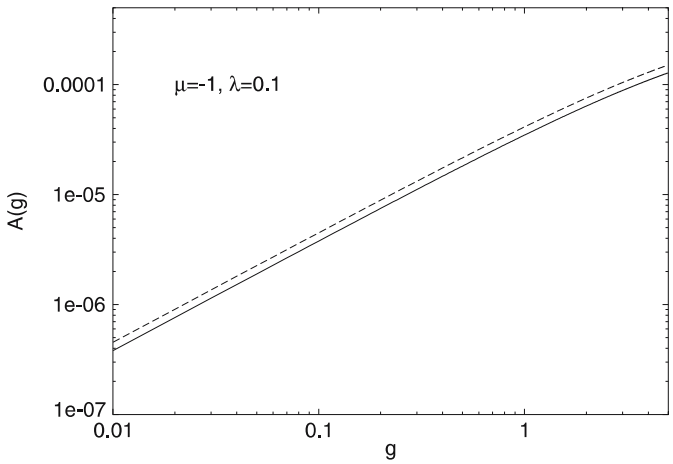

Fig. 8. The hA amplitude $A(y,g)$ at $y=10$ for $\mu=-1$, $\lambda=0.1$ (*lower curve*) as compared to the pure fan prediction (*upper curve*)

expects a similar saturation, but at higher values of g, as will become clear in the following.

We again compare our exact results with the predictions of the pure fan approximation, (53) with $g_{\rm i}=1$ and $u=g$, and the asymptotic formula similar to (111):

$$A(y,g)=\varrho\Big(1-\mathrm{e}^{-g\varrho}\Big)\,\mathrm{e}^{-y\Delta E}\,. \qquad (112)$$

The results are shown in Figs. 6–8 for $(\mu,\lambda)=(1,1/10)$, $(1,1/3)$ and $(-1,1/10)$, respectively. With μ positive, the effect of the loops is considerable, so that the pure fan model gives a bad description, especially at low values of g and not very small values of λ. The asymptotic formula (120) works much better. At $\mu=1$ and $\lambda=1/10$ it gives very good results, as seen from Fig. 6. However, at larger values of λ/μ its precision rapidly goes down. The case with $\mu=-1$ and $\lambda=1/10$ illustrated in Fig. 8 was chosen to see the influence of loops for the subcritical pomeron, where such an influence should be minimal. In this case the pure

fan formula gives the amplitude

$$A(y=10,g) = \frac{g\,\mathrm{e}^{-y}}{1+10g(1-\mathrm{e}^{-y})}\Big|_{y=10}, \qquad (113)$$

which grows linearly with g up to values around $g = 10$ and only then saturates at the value $0.1\,\mathrm{e}^{-10}$. This explains the somewhat exceptional behavior of $A(y = 10, g)$ for such μ and λ. As it follows from Fig. 8, the influence of loops is in fact small. However, it is greater than $\sim \lambda^2 = 1\%$, as one could expect by simple estimates of a single loop contribution. In fact, the pure fan formula overshoots the exact result by about 20%.

8 Conclusions

As mentioned, zero-dimensional RFT was studied in detail some thirty years ago. Our aim was to clarify some mathematical aspects of the model, and also to study it at different values of the triple-pomeron coupling and not only at small ones.

We have found that the model can be consistently formulated in terms of a quantum Hamiltonian. This formulation is valid both for negative and positive values of μ, in contrast to the functional approach, which does not admit positive μ. The Hamiltonian formulation does not need the introduction of a scalar product in the representation in which the creation operators u are diagonal. The wave functions seem to be not integrable in the whole complex u-plane. Rather the standard scalar product should be used in which the creation and annihilation operators are expressed by Hermitean operators.

The physical content of the theory is clearly seen after the transformation to an Hermitean Hamiltonian made in [6]. However, such a transformation can only be done separately for positive and negative u, leading to two branches of the spectrum for the initial Hamiltonian, which include both positive and negative eigenvalues. The choice between the two branches is determined by the signs of λ and the external coupling constants.

For $\mu > 0$ the simple case of pure fan diagrams admits an explicit solution and a reinterpretation in terms of the probabilistic approach. Using this, one can obtain an approximate expression for the pomeron propagator with loops of the largest extension in rapidity taken into account, which gives a reasonable approximation at small values of λ.

Finally, we performed numerical calculations of the amplitudes. They show that in all cases the triple-pomeron interaction makes the amplitudes fall at high rapidities. This fall starts later for smaller λ and at very small λ begins at asymptotically high rapidities (for $\lambda/\mu < 1/4$ it is noticeable only at $\mu y > 100$). At small λ, the behavior in y is well described by formulas obtained in earlier studies. However, when λ is not so small all approximate formulas work poorly. Our numerical calculations have also shown that there is no visible singularity at $\mu = 0$, in spite of the fact that the functional formulation meets with a divergence at this point.

We have proposed a new method for the perturbative treatment of the theory, which may have applications to more sophisticated models in the world of more dimensions

Acknowledgements. M.A.B. and G.P.V. gratefully acknowledge the hospitality of the II Institut for Theoretical Physics of the University of Hamburg, where part of this work was done. M.A.B. also thanks the Bologna Physics department and INFN for hospitality. The authors thank J. Bartels, S. Bondarenko, L. Motyka and A.H. Mueller for very interesting and constructive discussions. G.P.V. thanks the Alexander Von Humboldt foundation for partial support. This work was also partially supported by grants RNP 2.1.1.1112 and RFFI 06-02-16115a of Russia.

References

1. A.H. Mueller, Nucl. Phys. B **437**, 107 (1995)
2. A.H. Mueller, G.P. Salam, Nucl. Phys. B **475**, 293 (1996)
3. A. Schwimmer, Nucl. Phys. B **94**, 445 (1975)
4. D. Amati, L. Caneshi, R. Jengo, Nucl. Phys. B **101**, 397 (1975)
5. V. Alessandrini, D. Amati, R. Jengo, Nucl. Phys. B **108**, 425 (1976)
6. R. Jengo, Nucl. Phys. B **108**, 447 (1976)
7. D. Amati, M. Le Bellac, G. Marchesini, M. Ciafaloni, Nucl. Phys. **112**, 107 (1976)
8. M. Ciafaloni, M. Le Bellac, G.C. Rossi, Nucl. Phys. **130**, 388 (1977)
9. M. Ciafaloni, Nucl. Phys. B **146**, 427 (1978)
10. K.G. Boreskov, arXiv:hep-ph/0112325
11. S. Bondarenko, L. Motyka, A.H. Mueller, A.I. Shoshi, B.-W. Xiao, arXiv:hep-ph/0609213
12. M. Kozlov, E. Levin, Nucl. Phys. A **779**, 142 (2006)
13. M. Kozlov, E. Levin, V. Khachatryan, J. Miller, arXiv:hep-ph/0610084
14. G.P. Salam, Nucl. Phys. B **461**, 512 (1996)
15. Y.V. Kovchegov, Phys. Rev. D **72**, 094 009 (2005)
16. C.M. Bender, S. Boettcher, Phys. Rev. Lett. **80**, 5243 (1998)
17. C.M. Bender, D.C. Brody, H.F. Jones, Phys. Rev. Lett. **89**, 270 401 (2002) [Erratum ibid. **92**, 119902 (2004)]
18. A. Mostafazadeh, J. Math. Phys. **43**, 3944 (2002)
19. A. Mostafazadeh, J. Phys. A **38**, 6557 (2005) [Erratum ibid. A **38**, 8185 (2005)]